

Shear viscosity in antikaon condensed matter

Rana Nandi¹, Sarmistha Banik² and Debades Bandyopadhyay¹

¹*Theory Division and Centre for Astroparticle Physics,*

Saha Institute of Nuclear Physics, 1/AF Bidhannagar, Kolkata-700064, India and

²*Variable Energy Cyclotron Centre,*

1/AF Bidhannagar, Kolkata-700064, India

Abstract

We investigate the shear viscosity of neutron star matter in the presence of an antikaon condensate. The electron and muon number densities are reduced due to the appearance of a K^- condensate in neutron star matter, whereas the proton number density increases. Consequently the shear viscosity due to scatterings of electrons and muons with themselves and protons is lowered compared to the case without the condensate. On the other hand, the contribution of proton-proton collisions to the proton shear viscosity through electromagnetic and strong interactions, becomes important and comparable to the neutron shear viscosity.

PACS numbers: 97.60.Jd, 26.60.-c, 52.25.Fi, 52.27.Ny

I. INTRODUCTION

Shear viscosity plays important roles in neutron star physics. It might damp the r-mode instability below the temperature $\sim 10^8$ K [1]. The knowledge of shear viscosity is essential in understanding pulsar glitches and free precession of neutron stars [2]. The calculation of the neutron shear viscosity (η_n) for nonsuperfluid matter using free-space nucleon-nucleon scattering data was first done by Flowers and Itoh [3, 4]. Cutler and Lindblom [5] fitted the results of Flowers and Itoh [4] for the study of viscous damping of oscillations in neutron stars. Recently the neutron shear viscosity of pure neutron matter has been investigated in a self-consistent way [6].

It was noted that electrons, the lightest charged particles and neutrons, the most abundant particles in neutron star matter contribute significantly to the total shear viscosity. Flowers and Itoh found that the neutron viscosity was larger than the combined viscosity of electrons and muons ($\eta_{e\mu}$) in non-superfluid matter [4]. Further Cutler and Lindblom argued that the electron viscosity was larger than the neutron viscosity in a superfluid neutron star [5]. Later Andersson and his collaborators as well as Yakovlev and his collaborator showed $\eta_{e\mu} > \eta_n$ in the presence of proton superfluidity [2, 7]. In the latter calculation, the effects of the exchange of transverse plasmons in the collisions of charged particles were included and it lowered the $\eta_{e\mu}$ compared with the case when only longitudinal plasmons were considered [7].

So far, all of those calculations of shear viscosity were done in neutron star matter composed of neutrons, protons, electrons and muons. However, exotic forms of matter such as hyperon or antikaon condensed matter might appear in the interior of neutron stars. Negatively charged hyperons or a K^- condensate could affect the electron shear viscosity appreciably.

Here we focus on the role of K^- meson condensates on the shear viscosity. No calculation of shear viscosity involving antikaon condensation has been carried out so far. This motivates us to investigate the shear viscosity in the presence of an antikaon condensate. The K^- condensate appears at 2-3 times the normal nuclear matter density. With the onset of the condensate, K^- mesons replace electrons and muons in the core. As a result, K^- mesons along with protons maintain the charge neutrality. It was noted that the proton fraction became comparable to the neutron fraction in a neutron star including the K^- condensate

at higher densities [8, 9, 10]. The appearance of the K^- condensate would not only influence the electron and muon shear viscosities but it will also give rise to a new contribution called the proton shear viscosity.

This paper is organised in the following way. In Sec. II, we describe the calculation of shear viscosity in neutron stars involving the K^- condensate. Results are discussed in Sec. III. A summary is given in Sec. IV.

II. FORMALISM

Here we are interested in calculating the shear viscosity of neutron star matter in the presence of an antikaon condensate. We consider neutron star matter undergoing a first order phase transition from charge neutral and beta-equilibrated nuclear matter to a K^- condensed phase. The nuclear phase is composed of neutrons, protons, electrons and muons whereas the antikaon condensed phase is made up of neutrons and protons embedded in the Bose-Einstein condensate of K^- mesons along with electrons and muons. Antikaons form a s-wave ($\mathbf{p} = \mathbf{0}$) condensation in this case. Therefore, K^- mesons in the condensate do not take part in momentum transfer during collisions with other particles. However, the condensate influences the proton fraction and equation of state (EOS) which, in turn, might have important consequences for the shear viscosity. The starting point for the calculation of the shear viscosity is a set of coupled Boltzmann transport equations [4, 7] for the i th particle species ($i = n, p, e, \mu$) with velocity v_i and distribution function F_i ,

$$\vec{v}_i \cdot \vec{\nabla} F_i = \sum_{j=n,p,e,\mu} I_{ij}. \quad (1)$$

The transport equations are coupled through collision integrals given by,

$$I_{ij} = \frac{V^3}{(2\pi\hbar)^9(1 + \delta_{ij})} \sum_{s_i, s_j, s_{i'}} \int d\mathbf{p}_j d\mathbf{p}_{i'} d\mathbf{p}_{j'} W_{ij} \mathcal{F}, \quad (2)$$

where

$$\mathcal{F} = [F_{i'} F_{j'} (1 - F_i)(1 - F_j) - F_i F_j (1 - F_{i'})(1 - F_{j'})]. \quad (3)$$

Here $\mathbf{p}_i, \mathbf{p}_j$ are momenta of incident particles and $\mathbf{p}_{i'}, \mathbf{p}_{j'}$ are those of final states. The Kronecker delta in Eq. (2) is inserted to avoid double counting for identical particles. Spins are denoted by s and W_{ij} is the differential transition rate. The nonequilibrium distribution

function for the i -th species F_i is given by

$$F_i = f_i - \phi_i \frac{\partial f_i}{\partial \epsilon_i}, \quad (4)$$

where the equilibrium Fermi-Dirac distribution function $f(\epsilon_i) = \frac{1}{1 + e^{\frac{\epsilon_i - \mu_i}{kT}}}$ and the departure from the equilibrium is given by ϕ . We adopt the following ansatz for ϕ_i [7, 11]

$$\phi_i = -\tau_i (v_i p_j - \frac{1}{3} v_i p_i \delta_{ij}) (\nabla_i \mathcal{V}_j + \nabla_j \mathcal{V}_i - \frac{2}{3} \delta_{ij} \vec{\nabla} \cdot \vec{\mathcal{V}}), \quad (5)$$

where τ_i is the effective relaxation time for the i th species and \mathcal{V} is the flow velocity. The transport equations are linearised and multiplied by $(2\pi\hbar)^{-3} (v_i p_j - \frac{1}{3} v_i p_i \delta_{ij}) d\mathbf{p}_i$. Summing over spin s_i and integrating over $d\mathbf{p}_i$ we obtain a set of relations between effective relaxation times and collision frequencies [7]

$$\sum_{j=n,p,e,\mu} (\nu_{ij} \tau_i + \nu'_{ij} \tau_j) = 1, \quad (6)$$

and the effective collision frequencies are

$$\begin{aligned} \nu_{ij} = \frac{3\pi^2 \hbar^3}{2p_{F_i}^5 kT m_i^* (1 + \delta_{ij})} \sum_{s_i, s_{i'}, s_j, s_{j'}} \int \frac{d\mathbf{p}_i d\mathbf{p}_j d\mathbf{p}_{i'} d\mathbf{p}_{j'}}{(2\pi\hbar)^{12}} W_{ij} [f_i f_j (1 - f_{i'}) (1 - f_{j'})] \\ \times [\frac{2}{3} p_i^4 + \frac{1}{3} p_i^2 p_{i'}^2 - (\mathbf{p}_i \cdot \mathbf{p}_{i'})^2], \end{aligned} \quad (7)$$

$$\begin{aligned} \nu'_{ij} = \frac{3\pi^2 \hbar^3}{2p_{F_i}^5 kT m_j^* (1 + \delta_{ij})} \sum_{s_i, s_{i'}, s_j, s_{j'}} \int \frac{d\mathbf{p}_i d\mathbf{p}_j d\mathbf{p}_{i'} d\mathbf{p}_{j'}}{(2\pi\hbar)^{12}} W_{ij} [f_i f_j (1 - f_{i'}) (1 - f_{j'})] \\ \times [\frac{1}{3} p_i^2 p_{j'}^2 - \frac{1}{3} p_i^2 p_j^2 + (\mathbf{p}_i \cdot \mathbf{p}_j)^2 - (\mathbf{p}_i \cdot \mathbf{p}_{j'})^2]. \end{aligned} \quad (8)$$

The differential transition rate is given by

$$\sum_{s_i, s_{i'}, s_j, s_{j'}} W_{ij} = 4(2\pi)^4 \hbar^2 \delta(\epsilon_i + \epsilon_j - \epsilon_{i'} - \epsilon_{j'}) \delta(\mathbf{p}_i + \mathbf{p}_j - \mathbf{p}_{i'} - \mathbf{p}_{j'}) \mathcal{Q}_{ij}, \quad (9)$$

where $\mathcal{Q}_{ij} = \langle |\mathcal{M}_{ij}|^2 \rangle$ is the squared matrix element summed over final spins and averaged over initial spins [7, 12, 13].

We obtain effective relaxation times for different particle species solving a matrix equation that follows from Eq.(6). The matrix equation has the following form:

$$\begin{pmatrix} \nu_e & \nu'_{e\mu} & \nu'_{ep} & 0 \\ \nu'_{\mu e} & \nu_\mu & \nu'_{\mu p} & 0 \\ \nu'_{pe} & \nu'_{p\mu} & \nu_p & \nu'_{pn} \\ 0 & 0 & \nu'_{np} & \nu_n \end{pmatrix} \begin{pmatrix} \tau_e \\ \tau_\mu \\ \tau_p \\ \tau_n \end{pmatrix} = 1 \quad (10)$$

where,

$$\nu_e = \nu_{ee} + \nu'_{ee} + \nu_{e\mu} + \nu_{ep} , \quad (11)$$

$$\nu_\mu = \nu_{\mu\mu} + \nu'_{\mu\mu} + \nu_{\mu e} + \nu_{\mu p} , \quad (12)$$

$$\nu_p = \nu_{pp} + \nu'_{pp} + \nu_{pn} + \nu_{pe} + \nu_{p\mu} , \quad (13)$$

$$\nu_n = \nu_{nn} + \nu'_{nn} + \nu_{np} . \quad (14)$$

It is to be noted here that the proton-proton interaction is made up of contributions from electromagnetic and strong interactions. As there is no interference of the electromagnetic and strong interaction terms, the differential transition rate for the proton-proton scattering is the sum of electromagnetic and strong contributions. This was discussed earlier in Ref.[4]. Therefore, we can write the strong and electromagnetic parts of the effective collision frequencies of proton-proton scattering as

$$\begin{aligned} \nu_{pp} &= \nu_{pp}^s + \nu_{pp}^{em} , \\ \nu'_{pp} &= \nu'^s_{pp} + \nu'^{em}_{pp} . \end{aligned} \quad (15)$$

Here the superscripts 'em' and 's' denote the electromagnetic and strong interactions. Solutions of Eq. (10) are given below

$$\begin{aligned} \tau_e &= \frac{(\nu_p \nu_n - \nu'_{pn} \nu'_{np})(\nu_\mu - \nu'_{e\mu}) + (\nu'_{pn} - \nu_n)(\nu_\mu \nu'_{ep} - \nu'_{e\mu} \nu'_{\mu p}) + \nu_n \nu'_{p\mu} (\nu'_{ep} - \nu'_{\mu p})}{\det A} , \\ \tau_p &= \frac{(\nu_n - \nu'_{pn})(\nu_e \nu_\mu - \nu'_{e\mu} \nu'_{\mu e}) + \nu'_{p\mu} \nu_n (\nu'_{e\mu} - \nu_e) + \nu'_{pe} \nu_n (\nu'_{e\mu} - \nu_\mu)}{\det A} , \\ \tau_n &= \frac{(\nu_p - \nu'_{np})(\nu_e \nu_\mu - \nu'_{e\mu} \nu'_{\mu e}) + (\nu'_{np} - \nu'_{\mu p})(\nu'_{p\mu} \nu_e - \nu'_{e\mu} \nu'_{p\mu}) + (\nu'_{ep} - \nu'_{np})(\nu'_{\mu e} \nu'_{p\mu} - \nu'_{pe} \nu_\mu)}{\det A} \end{aligned} \quad (16)$$

where A is the 4×4 matrix of Eq. (10) and $\det A = [\nu_e \nu_\mu (\nu_p \nu_n - \nu'_{pn} \nu'_{np}) - \nu_e \nu'_{\mu p} \nu'_{p\mu} \nu_n - \nu'_{e\mu} \nu'_{\mu e} (\nu_p \nu_n - \nu'_{pn} \nu'_{np}) - \nu'_{e\mu} \nu'_{\mu p} \nu'_{pe} \nu_n + \nu'_{ep} \nu'_{\mu e} \nu'_{p\mu} \nu_n - \nu'_{ep} \nu_\mu \nu'_{pe} \nu_n]$. We obtain τ_μ from τ_e replacing e by μ . In the next paragraphs, we discuss the determination of matrix element squared for electromagnetic and strong interactions.

First we focus on the electromagnetic scattering of charged particles. Here we adopt the plasma screening of the interaction due to the exchange of longitudinal and transverse plasmons as described in Refs.[7, 12, 14]. The matrix element for the collision of identical charged particles is given by $M_{12} = M_{12}^{(1)} + M_{12}^{(2)}$, where the first term implies the scattering channel $12 \rightarrow 1'2'$ and the second term corresponds to that of $12 \rightarrow 2'1'$. The scattering of

charged particles in neutron star interiors involves small momentum and energy transfers. Consequently both channels contribute equally because the interference term is small in this case. The matrix element for nonidentical particles is given by [7, 12, 14]

$$M_{12 \rightarrow 1'2'} = \frac{4\pi e^2}{c^2} \left(\frac{J_0^{11'} J_0^{22'}}{q^2 + \Pi_l^2} - \frac{\mathbf{J}_t^{11'} \cdot \mathbf{J}_t^{22'}}{q^2 - \omega^2/c^2 + \Pi_t^2} \right), \quad (17)$$

where \mathbf{q} and ω are momentum and energy transfers in the neutron star interior. Further four-current (J_0, \mathbf{J}) and longitudinal and transverse polarization functions (Π_l, Π_t) have the same expressions as defined in Ref.[7]. It is to be noted that \mathbf{J}_t is the transverse component of \mathbf{J} with respect to \mathbf{q} and the longitudinal component is related to the timelike component J_0 by the conservation of current [14]. Polarization functions Π_l and Π_t are associated with the plasma screening of charged particles' interactions through the exchange of longitudinal and transverse plasmons, respectively. After evaluating the matrix element squared and doing the angular and energy integrations, the effective collision frequencies are calculated following the prescription of Ref.[7, 12]. The collision frequencies of Eqs. (7) and (8) for charged particles become

$$\begin{aligned} \nu_{ij} &= \nu_{ij}^{\parallel} + \nu_{ij}^{\perp}, \\ \nu'_{ij} &= \nu'^{\parallel\perp}_{ij}, \end{aligned} \quad (18)$$

where ν_{ij}^{\parallel} and ν_{ij}^{\perp} correspond to the charged particle interaction due to the exchange of longitudinal and transverse plasmons and $\nu'^{\parallel\perp}_{ij}$ is the result of the interference of both interactions. For small momentum and energy transfers, different components of the collision frequency are given by [7, 12]

$$\begin{aligned} \nu_{ij}^{\perp} &= \frac{e^4 \alpha}{\hbar^4 c^3} \frac{p_{F_j}^2}{p_{F_i} m_i^* c} \left(\frac{\hbar c}{q_t^2} \right)^{1/3} (kT)^{5/3}, \\ \nu_{ij}^{\parallel} &= \frac{e^4 \pi^2 m_i^* m_j^{*2}}{\hbar^4 p_{F_i}^3 q_l} (kT)^2, \\ \nu'^{\parallel\perp}_{ij} &= \frac{2e^4 \pi^2 m_i^* p_{F_j}^2}{\hbar^4 c^2 p_{F_i}^3 q_l} (kT)^2, \end{aligned} \quad (19)$$

where $i, j = e, \mu, p$ and longitudinal and transverse wave numbers are given by

$$\begin{aligned} q_l^2 &= \frac{4e^2}{\hbar^3 c \pi} \sum_{j=e, \mu, p} c m_j^* p_{F_j}, \\ q_t^2 &= \frac{4e^2}{\hbar^3 c \pi} \sum_{j=e, \mu, p} p_{F_j}^2. \end{aligned} \quad (20)$$

The value of $\alpha = 2(\frac{4}{\pi})^{1/3}\Gamma(8/3)\zeta(5/3) \sim 6.93$ where $\Gamma(x)$ and $\zeta(x)$ are gamma and Riemann zeta functions, respectively. The shear viscosities of electrons and muons are given by [7]

$$\eta_{i(=e,\mu)} = \frac{n_i p_{F_i}^2 \tau_i}{5m_i^*} . \quad (21)$$

Here effective masses (m_i^*) of electrons and muons are equal to their corresponding chemical potentials because of relativistic effects. It was noted that the shear viscosity was reduced due to the inclusion of plasma screening by the exchange of transverse plasmons [7, 12]. It is worth mentioning here that we extend the calculation of the collision frequencies for electrons and muons in Refs.[7, 12] to that of protons due to electromagnetic interaction. Before the appearance of the condensate in our calculation, protons may be treated as passive scatterers as was earlier done by Ref.[7]. However, after the onset of the antikaon condensation, electrons and muons are replaced by K^- mesons and proton fraction increases rapidly in the system [9, 10]. In this situation protons can not be treated as passive scatterers.

Next we focus on the calculation of collision frequencies of neutron-neutron, proton-proton and neutron-proton scatterings due to the strong interaction. The knowledge of nucleon-nucleon scattering cross sections are exploited in this calculation. This was first done by Ref.[4]. Later recent developments in the calculation of nucleon-nucleon scattering cross sections in the Dirac-Brueckner approach were considered for this purpose [12, 13]. Here we adopt the same prescription of Ref.[13] for the calculation of collision frequencies due to nucleon-nucleon scatterings. The collision frequency for the scattering of identical particles under strong interaction is given by

$$\nu_{ii} + \nu'_{ii} = \frac{16m_i^{*3}(kT)^2}{3m_n^2\hbar^3} S_{ii} , \quad (22)$$

$$S_{ii} = \frac{m_n^2}{16\hbar^4\pi^2} \int_0^1 dx' \int_0^{\sqrt{(1-x'^2)}} dx \frac{12x^2x'^2}{\sqrt{1-x^2-x'^2}} \mathcal{Q}_{ii} , \quad (23)$$

where $i = n, p$ and m_n is the bare nucleon mass and \mathcal{Q}_{ii} is the matrix element squared which appears in Eq. (9). Similarly we can write the collision frequency for nonidentical particles as

$$\begin{aligned} \nu_{ij} &= \frac{32m_i^*m_j^{*2}(kT)^2}{3m_n^2\hbar^3} S_{ij} , \\ \nu'_{ij} &= \frac{32m_i^{*2}m_j^*(kT)^2}{3m_n^2\hbar^3} S'_{ij} , \end{aligned} \quad (24)$$

and

$$\begin{aligned}
S_{ij} &= \frac{m_n^2}{16\hbar^4\pi^2} \int_{0.5-x_0}^{0.5+x_0} dx' \int_0^f dx \frac{6(x^2 - x^4)}{\sqrt{(f^2 - x^2)}} \mathcal{Q}_{ij} , \\
S'_{ij} &= \frac{m_n^2}{16\hbar^4\pi^2} \int_{0.5-x_0}^{0.5+x_0} dx' \int_0^f dx \frac{[6x^4 + 12x^2x'^2 - (3 + 12x_0^2)x^2]}{\sqrt{(f^2 - x^2)}} \mathcal{Q}_{ij} .
\end{aligned} \tag{25}$$

We define $x_0 = \frac{p_{F_j}}{2p_{F_i}}$, $x = \frac{\hbar q}{2p_{F_i}}$, $x' = \frac{\hbar q'}{2p_{F_i}}$, $f = \frac{\sqrt{x_0^2 - (0.25 + x_0^2 - x'^2)^2}}{x'}$, where momentum transfers $\mathbf{q} = \mathbf{p}_{j'} - \mathbf{p}_j$ and $\mathbf{q}' = \mathbf{p}_{j'} - \mathbf{p}_i$. We find that the calculation of S_{ij} , S_{ii} and S'_{ij} requires the knowledge of \mathcal{Q}_{ii} and \mathcal{Q}_{ij} . The matrix elements squared may be extracted from nucleon-nucleon differential cross sections. A detailed discussion on the calculation of matrix elements squared from the in-vacuum nucleon-nucleon differential scattering cross sections computed using Dirac-Brueckner approach [15, 16] can be found in Ref.[12, 13]. We follow this procedure in this calculation. It is to be noted here that S_{pp} , S_{pn} and S'_{ij} are the new results of this calculation. As soon as we know the collision frequencies of nucleon-nucleon scatterings due to the strong interaction, we can immediately calculate effective relaxation times of neutrons and protons from Eq. (16). This leads to the calculation of the neutron and proton shear viscosities as

$$\begin{aligned}
\eta_n &= \frac{n_n p_{F_n}^2 \tau_n}{5m_n^*} , \\
\eta_p &= \frac{n_p p_{F_p}^2 \tau_p}{5m_p^*} .
\end{aligned} \tag{26}$$

Finally the total shear viscosity is given by

$$\eta_{total} = \eta_n + \eta_p + \eta_e + \eta_\mu . \tag{27}$$

The EOS enters into the calculation of the shear viscosity as an input. We construct the EOS within the framework of the relativistic field theoretical model [17, 18]. Here we consider a first order phase transition from nuclear matter to K^- condensed matter. We adopt the Maxwell construction for the first order phase transition. The constituents of matter are neutrons, protons, electrons and muons in both phases and also (anti)kaons in the K^- condensed phase. Both phases maintain charge neutrality and β equilibrium conditions. Baryons and (anti)kaons are interacting with each other and among themselves by the exchange of σ , ω and ρ mesons [9, 10]. The baryon-baryon interaction is given by

the Lagrangian density [19, 20]

$$\begin{aligned}
\mathcal{L}_B = & \sum_{B=n,p} \bar{\psi}_B (i\gamma_\mu \partial^\mu - m_B + g_{\sigma B} \sigma - g_{\omega B} \gamma_\mu \omega^\mu - g_{\rho B} \gamma_\mu \mathbf{t}_B \cdot \boldsymbol{\rho}^\mu) \psi_B \\
& + \frac{1}{2} (\partial_\mu \sigma \partial^\mu \sigma - m_\sigma^2 \sigma^2) - U(\sigma) \\
& - \frac{1}{4} \omega_{\mu\nu} \omega^{\mu\nu} + \frac{1}{2} m_\omega^2 \omega_\mu \omega^\mu - \frac{1}{4} \boldsymbol{\rho}_{\mu\nu} \cdot \boldsymbol{\rho}^{\mu\nu} + \frac{1}{2} m_\rho^2 \boldsymbol{\rho}_\mu \cdot \boldsymbol{\rho}^\mu .
\end{aligned} \tag{28}$$

The scalar self-interaction [19, 20, 21] is

$$U(\sigma) = \frac{1}{3} g_1 m_N (g_{\sigma N} \sigma)^3 + \frac{1}{4} g_2 (g_{\sigma N} \sigma)^4 , \tag{29}$$

The effective nucleon mass is given by $m_B^* = m_B - g_{\sigma B} \sigma$, where m_B is the vacuum baryon mass. The Lagrangian density for (anti)kaons in the minimal coupling is given by [9, 10, 22]

$$\mathcal{L}_K = D_\mu^* \bar{K} D^\mu K - m_K^{*2} \bar{K} K , \tag{30}$$

where the covariant derivative is $D_\mu = \partial_\mu + i g_{\omega K} \omega_\mu + i g_{\rho K} \mathbf{t}_K \cdot \boldsymbol{\rho}_\mu$ and the effective mass of (anti)kaons is $m_K^* = m_K - g_{\sigma K} \sigma$. The in-medium energies of K^\pm mesons are given by

$$\omega_{K^\pm} = \sqrt{(p^2 + m_K^{*2})} \pm \left(g_{\omega K} \omega_0 + \frac{1}{2} g_{\rho K} \rho_{03} \right) . \tag{31}$$

The condensation sets in when the chemical potential of K^- mesons ($\mu_{K^-} = \omega_{K^-}$) is equal to the electron chemical potential i.e. $\mu_e = \mu_{K^-}$.

Using the mean field approximation [17, 18] and solving equations of motion self-consistently, we calculate the effective nucleon mass and Fermi momenta of particles at different baryon densities.

III. RESULTS AND DISCUSSIONS

The knowledge of meson-nucleon and meson-kaon coupling constants are needed for this calculation. The nucleon-meson coupling constants determined by reproducing the nuclear matter saturation properties such as binding energy $E/B = -16.3$ MeV, baryon density $n_0 = 0.153 \text{ fm}^{-3}$, the asymmetry energy coefficient $a_{\text{asy}} = 32.5$ MeV, incompressibility $K = 300$ MeV, and effective nucleon mass $m_N^*/m_N = 0.70$, are taken from Ref.[23]. Next we determine the kaon-meson coupling constants using the quark model and isospin counting rule. The vector coupling constants are given by

$$g_{\omega K} = \frac{1}{3} g_{\omega N} \quad \text{and} \quad g_{\rho K} = g_{\rho N} . \tag{32}$$

The scalar coupling constant is obtained from the real part of K^- optical potential depth at normal nuclear matter density

$$U_{\bar{K}}(n_0) = -g_{\sigma K}\sigma - g_{\omega K}\omega_0 . \quad (33)$$

It is known that antikaons experience an attractive potential and kaons have a repulsive interaction in nuclear matter [24, 25, 26, 27, 28, 29]. On the one hand, the analysis of K^- atomic data indicated that the real part of the antikaon optical potential could be as large as $U_{\bar{K}} = -180 \pm 20$ MeV at normal nuclear matter density [24, 25]. On the other hand, chirally motivated coupled channel models with a self-consistency requirement predicted shallow potential depths of -40 - 60 MeV [30, 31]. Recently, the double pole structure of $\Lambda(1405)$ was investigated in connection with the antikaon-nucleon interaction [32, 33]. Further, the highly attractive potential depth of several hundred MeV was obtained in the calculation of deeply bound antikaon-nuclear states [34, 35]. An alternative explanation to the deeply bound antikaon-nuclear states was given by others [36]. This shows that the value of antikaon optical potential depth is still a debatable issue. Motivated by the findings of the analysis of K^- atomic data, we perform this calculation for an antikaon optical potential depth $U_{\bar{K}} = -160$ MeV at normal nuclear matter density. We obtain kaon-scalar meson coupling constant $g_{\sigma K} = 2.9937$ corresponding to $U_{\bar{K}}(n_0) = -160$ MeV.

The composition of neutron star matter including the K^- condensate as a function of normalised baryon density is shown in Fig. 1. The K^- condensation sets in at $2.43n_0$. Before the onset of the condensation, all particle fractions increase with baryon density. In this case, the charge neutrality is maintained by protons, electrons and muons. As soon as the antikaon condensate is formed, the density of K^- mesons in the condensate rapidly increases and K^- mesons replace leptons in the system. The proton density eventually becomes equal to the K^- density. The proton density in the presence of the condensate increases significantly and may be higher than the neutron density at higher baryon densities [29]. This increase in the proton fraction in the presence of the K^- condensate might result in an enhancement in the proton shear viscosity and appreciable reduction in the electron and muon viscosities compared with the case without the condensate. We discuss this in details in the following paragraphs.

Next we focus on the calculation of ν_{ii} , ν_{ij} and ν'_{ij} . For the scatterings via the electromagnetic interaction, we calculate those quantities using Eqs. (18) and (19). On the

other hand, ν s corresponding to collisions through the strong interaction are estimated using Eqs. (22)-(25). In an earlier calculation, the authors considered only S_{nn} and S_{np} [7] for the calculation of the neutron shear viscosity in nucleons-only neutron star matter because protons were treated as passive scatterers. It follows from the discussion in the preceding paragraph that protons can no longer be treated as passive scatterers because of the large proton fraction in the presence of the K^- condensate. Consequently the contributions of S_{pp} and S_{pn} have to be taken into account in the calculation of the proton and neutron shear viscosities. The expressions of S_{nn} , S_{pp} , S_{np} and S_{pn} given by Eqs. (23) and (25) involve matrix elements squared. We note that there is an one to one correspondence between the differential cross section and the matrix element squared [13]. We exploit the in-vacuum nucleon-nucleon cross sections of Li and Machleidt [15, 16] calculated using Bonn interaction in the Dirac-Brueckner approach for the calculation of matrix elements squared. We fit the neutron-proton as well as proton-proton differential cross sections and use them in Eqs. (23) and (25) to calculate S_{nn} , S_{pp} , S_{np} and S_{pn} which are functions of neutron (p_{F_n}) and proton (p_{F_p}) Fermi momenta. The values of p_{F_n} ranges from 1.3 to 2.03 fm^{-1} whereas that of p_{F_p} spans the interval 0.35 to 1.73 fm^{-1} . This corresponds to the density range ~ 0.5 to $\sim 3.0n_0$. We fit the results of our calculation. Figures 2 and 3 display the variation of S_{nn} , S_{pp} , S_{np} and S_{pn} with baryon density. The value of S_{nn} is greater than that of S_{np} in the absence of the condensate as evident from Fig. 2. Our results agree well with those of Ref.[7]. However, S_{np} rises rapidly with baryon density after the onset of the K^- condensation and becomes higher than S_{nn} . It is noted that the effect of the condensate on S_{nn} is not significant. Figure 3 shows that S_{pp} drops sharply with increasing baryon density and crosses the curve of S_{pn} in the absence of the condensate. However S_{pp} and S_{pn} are not influenced by the antikaon condensate. A comparison of Fig. 2 and Fig. 3 reveals that S_{pp} is almost one order of magnitude larger than S_{nn} at lower baryon densities. This may be attributed to the smaller proton Fermi momentum. We also compute S'_{np} and S'_{pn} (not shown here) and these quantities have negative values. Further we find that the magnitude of S'_{pn} is higher than that of S'_{np} . It is to be noted here that S'_{ij} is related to ν'_{ij} by Eq. (24). This is again connected to Eq. (6). Therefore, the values of S'_{ij} and ν'_{ij} can be made positive by putting a negative sign between two terms in Eq. (6).

As soon as we know ν s, we can calculate effective relaxation times using Eq. (16) and shear viscosities using Eqs. (21), (26) and (27). First, we discuss the total shear viscosity

in nuclear matter without a K^- condensate. This is shown as a function of baryon density at a temperature 10^8K in Fig. 4. Here our results indicated by the solid line are compared with the calculation of the total shear viscosity using the EOS of Akmal, Pandharipande and Ravenhall (APR) [37] denoted by the dotted line and also with the results of Flowers and Itoh [3, 4]. For the APR case, we exploit the parametrization of the EOS by Heiselberg and Hjorth-Jensen [38]. Further we take density independent nucleon effective masses $m_n^* = m_p^* = 0.8m_n$ for the calculation with the APR EOS which was earlier discussed by Shternin and Yakovlev [12]. On the other hand, the results of Flowers and Itoh were parametrized by Cutler and Lindblom (CL) [5] and it is shown by the dashed line in Fig. 4. It is evident from Fig. 4 that the total shear viscosity in our calculation is significantly higher than other cases. This may be attributed to the fact that our EOS is a fully relativistic one.

We exhibit shear viscosities in the presence of an antikaon condensate as a function of baryon density in Fig. 5. This calculation is performed at a temperature 10^8K . In the absence of the K^- condensate, the contribution of the electron shear viscosity to the total shear viscosity is the highest. The electron, muon and neutron shear viscosities exceed the proton shear viscosity by several orders of magnitude. Further we note that the lepton viscosities are greater than the neutron viscosity. On the other hand, we find interesting results in the presence of the antikaon condensate. The electron and muon shear viscosities decrease very fast after the onset of K^- condensation whereas the proton shear viscosity rises in this case. There is almost no change in the neutron shear viscosity. It is interesting to note that the proton shear viscosity in the presence of the condensate approaches the value of the neutron shear viscosity as baryon density increases. The total shear viscosity decreases in the K^- condensed matter due to the sharp drop in the lepton shear viscosities. Here the variation of shear viscosities with baryon density is shown up to $3n_0$. The neutron and proton shear viscosities in neutron star matter with the K^- condensate might dominate over the electron and muon shear viscosities beyond baryon density $3n_0$. Consequently, the total shear viscosity would again increase.

The temperature dependence of the total shear viscosity is shown in Fig. 6. In an earlier calculation, electron and muon shear viscosities were determined by collisions only due to the exchange of transverse plasmons because this was the dominant contribution [12]. Under this approximation, the electron and muon shear viscosities had a temperature dependence of $T^{-5/3}$, whereas, the neutron shear viscosity was proportional to T^{-2} . The temperature de-

pendence of the electron and muon shear viscosities deviated from the standard temperature dependence of the shear viscosity of neutron Fermi liquid. However, in this calculation we have not made any such approximation. We have considered all the components of effective collision frequency which have different temperature dependence as given by Eq. (19). This gives rise to a complicated temperature dependence in the calculation of shear viscosity. The total shear viscosity is plotted for $T = 10^7$, 10^8 , and 10^9 K in Fig. 6. It is noted that the shear viscosity increases as temperature decreases.

The shear viscosity plays an important role in damping the r-mode instability in old and accreting neutron stars [39, 40, 41, 42, 43]. The suppression of the instability is achieved by the competition of various time scales associated with gravitational radiation (τ_{GR}), hyperon bulk viscosity (τ_B), modified Urca bulk viscosity (τ_U), and shear viscosity (τ_{SV}). At high temperatures the bulk viscosity damp the r-mode instability. As neutron stars cool down, the bulk viscosity might not be the dominant damping mechanism. The shear viscosity becomes significant in the temperature regime $\leq 10^8$ K and might suppress the r-mode instability effectively.

In this calculation, we consider only the antikaon optical potential depth $U_{\bar{K}} = -160$ MeV. However, this calculation could be performed for other values of antikaon optical potential depths. As the magnitude of the K^- potential depth decreases, the threshold of the antikaon condensation is shifted to higher densities [9]. On the other hand, hyperons may also appear in neutron star matter around $2-3n_0$. Negatively charged hyperons might delay the onset of K^- condensation [19, 44, 45]. However, it was noted in an earlier calculation that Σ^- hyperons were excluded from the system because of repulsive Σ -nuclear matter interaction and Ξ^- hyperons might appear at very high baryon density [10]. However, the appearance of Λ hyperons could compete with the threshold of K^- condensation. If Λ hyperons appear before K^- condensation, the threshold of K^- condensation is shifted to higher baryon density because of softening in the equation of state due to Λ hyperons. But the qualitative results of the shear viscosity discussed above remain the same.

IV. SUMMARY AND CONCLUSIONS

We have investigated the shear viscosity in the presence of a K^- condensate. With the onset of K^- condensation, electrons and muons are replaced by K^- mesons rapidly. The

proton fraction also increases and eventually becomes equal to the neutron fraction in the K^- condensed neutron star matter. This has important consequences for the electron, muon and proton shear viscosities. We have found that the electron and muon shear viscosities drop steeply after the formation of the K^- condensate in neutron stars. On the other hand, the proton shear viscosity whose contribution to the total shear viscosity was negligible in earlier calculations [4, 7], now becomes significant in the presence of the K^- condensate. The proton shear viscosity would exceed the neutron as well as lepton shear viscosities beyond $3n_0$. The total viscosity would be dominated by the proton and neutron shear viscosities in this case. This calculation may be extended to neutron stars with strong magnetic fields.

It is worth mentioning here that we adopt the Maxwell construction for the first order phase transition in this calculation. Such a construction is justified if the surface tension between two phases is quite large [46]. Moreover the value of the surface tension between the nuclear and antikaon condensed phases or between the hadron and quark phases is not known correctly. Therefore, this problem could also be studied using the Gibbs construction [47].

Besides the role of shear viscosity in damping the r-mode instability as well as in pulsar glitches and free precession of neutron stars, it has an important contribution in the nucleation rate of bubbles in first order phase transitions. It was shown earlier that the shear viscosity might control the initial growth rate of a bubble [48, 49]. This needs further study in connection with antikaon condensation in neutron stars.

V. ACKNOWLEDGMENTS

We thank R. Machleidt for providing us with the tables of neutron-proton and proton-proton differential scattering cross sections. RN and DB thank the Alexander von Humboldt Foundation for the support under the Research Group Linkage programme. We also acknowledge the warm hospitality at the Frankfurt Institute for Advanced Studies where a part of this work was completed.

[1] N. Andersson and K.D. Kokkotas, Mon. Not. R. Astron. Soc. **299**, 1059 (1998); Int. J. Mod. Phys. **D10**, 381 (2001).

- [2] N. Andersson, G. L. Comer and K. Glampedakis, Nucl. Phys. **A763**, 212 (2005).
- [3] E. Flowers and N. Itoh, Astrophys. J. **206**, 218 (1976).
- [4] E. Flowers and N. Itoh, Astrophys. J. **230**, 847 (1979).
- [5] C. Cutler and L. Lindblom, Astrophys. J. **314**, 234 (1987).
- [6] O. Benhar and M. Valli, Phys. Rev. Lett. **99**, 232501 (2007).
- [7] P. S. Shternin and D. G. Yakovlev, Phys. Rev. **D78**, 063006 (2008).
- [8] H. A. Bethe and G. E. Brown, Ap. J. **445**, L129 (1995).
- [9] S. Pal, D. Bandyopadhyay and W. Greiner, Nucl. Phys. **A674**, 553 (2000).
- [10] S. Banik and D. Bandyopadhyay, Phys. Rev. **C64**, 055805 (2001).
- [11] G. Rupak and T. Schäfer, Phys. Rev. **A76**, 053607 (2007).
- [12] P. S. Shternin and D. G. Yakovlev, Phys. Rev. **D75**, 103004 (2007).
- [13] D. A. Baiko, P. Haensel and D. G. Yakovlev, Astron. Astrophys. **374**, 151 (2001).
- [14] H. Heiselberg and C. J. Pethick, Phys. Rev. **D48**, 2916 (1993).
- [15] G.Q. Li and R. Machleidt, Phys. Rev. **C48**, 1702 (1993).
- [16] G.Q. Li and R. Machleidt, Phys. Rev. **C49**, 566 (1994).
- [17] J. D. Walecka, Annals of Phys. **83**, 491 (1974).
- [18] B. D. Serot, Phys. Lett. **86B**, 146 (1979).
- [19] J. Schaffner and I. N. Mishustin, Phys. Rev. **C53**, 1416 (1996).
- [20] N. K. Glendenning, Phys. Lett. **B114**, 392 (1982).
- [21] J. Boguta and A. R. Bodmer, Nucl. Phys. **A292**, 413 (1977).
- [22] N.K. Glendenning and J. Schaffner-Bielich, Phys. Rev. **C60**, 025803 (1999).
- [23] N.K. Glendenning and S.A. Moszkowski, Phys. Rev. Lett. **67**, 2414 (1991).
- [24] E. Friedman, A. Gal and C.J. Batty, Nucl. Phys. **A579**, 518 (1994);
C.J. Batty, E. Friedman and A. Gal, Phys. Rep. **287**, 385 (1997).
- [25] E. Friedman, A. Gal, J. Mareš and A. Cieplý, Phys. Rev. **C60**, 024314 (1999).
- [26] V. Koch, Phys. Lett. **B337**, 7 (1994).
- [27] T. Waas and W. Weise, Nucl. Phys. **A625**, 287 (1997).
- [28] G.Q. Li, C.-H. Lee and G.E. Brown, Phys. Rev. Lett. **79**, 5214 (1997); Nucl. Phys. **A625**,
372 (1997).
- [29] S. Pal, C.M. Ko, Z. Lin and B. Zhang, Phys. Rev. **C62**, 061903(R) (2000).
- [30] A. Ramos and E. Oset, Nucl. Phys. **A671**, 481 (2000).

- [31] J. Schaffner-Bielich, V. Koch and M. Effenberger, Nucl. Phys. **A669**, 153 (2000).
- [32] V.K. Magas, E. Oset and A. Ramos, Phys. Rev. Lett. **95**, 052301 (2005).
- [33] T. Hyodo and W. Weise, Phys. Rev. **C77**, 035204 (2008).
- [34] Y. Akaishi and T. Yamazaki, Phys. Rev. **C65**, 044005 (2002).
- [35] Y. Akaishi, A. Dote and T. Yamazaki, Phys. Lett. **B613**, 140 (2005).
- [36] A. Ramos, V.K. Magas, E. Oset and H. Toki, Nucl. Phys. **A804**, 219 (2008).
- [37] A. Akmal, V.R. Pandharipande and D.G. Ravenhall, Phys. Rev. **C58**, 1804 (1998).
- [38] H. Heiselberg and M. Hjorth-Jensen, Astrophys. J. Lett. **525**, L45 (1999).
- [39] M. Nayyar and B.J. Owen, Phys. Rev. **D73**, 084001 (2006).
- [40] D. Chatterjee and D. Bandyopadhyay, Phys. Rev. **D74**, 023003 (2006).
- [41] D. Chatterjee and D. Bandyopadhyay, Phys. Rev. **D75**, 123006 (2007).
- [42] D. Chatterjee and D. Bandyopadhyay, Astrophys. J. **680**, 686 (2008).
- [43] D. Chatterjee and D. Bandyopadhyay, J. Phys. **G35**, 104078 (2008).
- [44] P.J. Ellis, R. Knorren and M. Prakash, Phys. Lett. **B349**, 11 (1995).
- [45] R. Knorren, M. Prakash and P.J. Ellis, Phys. Rev. **C52**, 3470 (1995).
- [46] M.G. Alford, K. Rajagopal, S. Reddy and F. Wilczek, Phys. Rev. **D64**, 074017 (2001).
- [47] N.K. Glendenning, Phys. Rev. **D46**, 1274 (1992).
- [48] L.P. Csernai and J.I. Kapusta, Phys. Rev. **D46**, 1379 (1992).
- [49] I. Bombaci, D. Logoteta, P.K. Panda, C. Providencia and I. Vidana Phys. Lett. **B680**, 448 (2009).

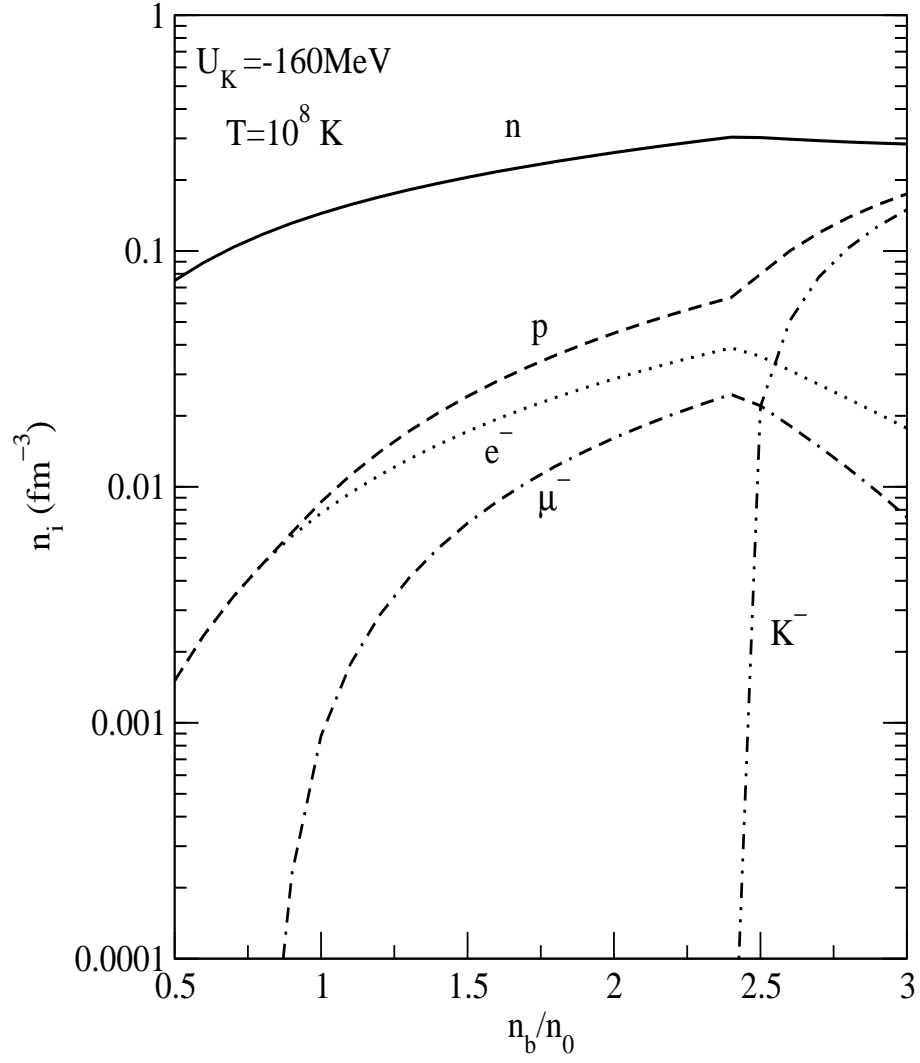


Fig. 1. Number densities of different particle species as a function of normalised baryon density.

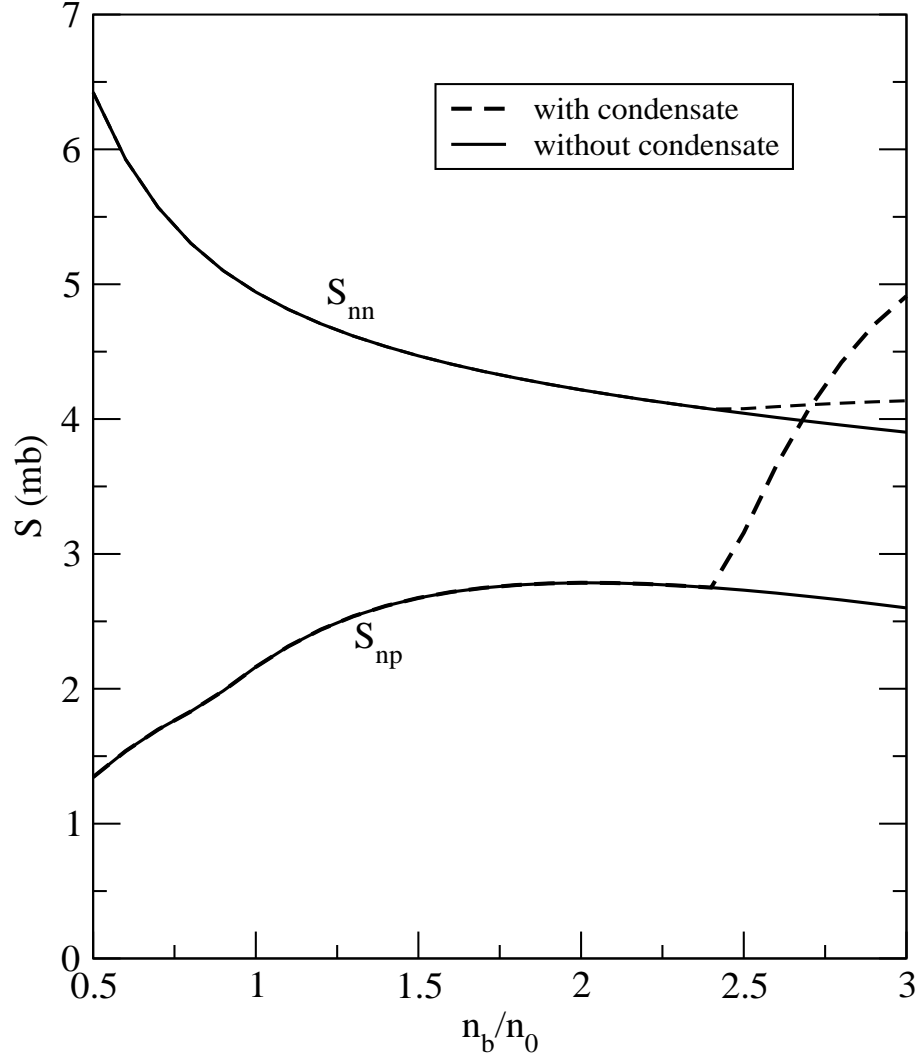


Fig. 2. S_{nn} and S_{np} are plotted as a function of normalised baryon density.

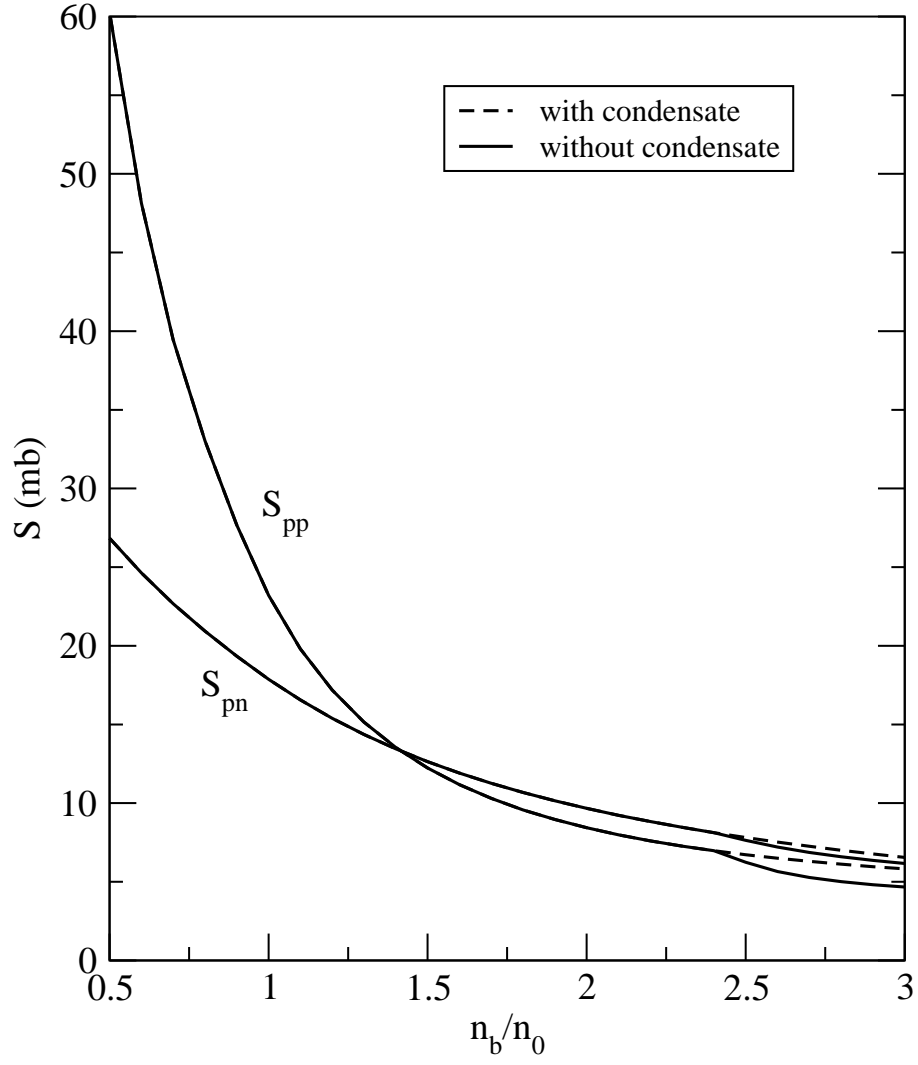


Fig. 3. S_{pp} and S_{pn} are plotted as a function of normalised baryon density.

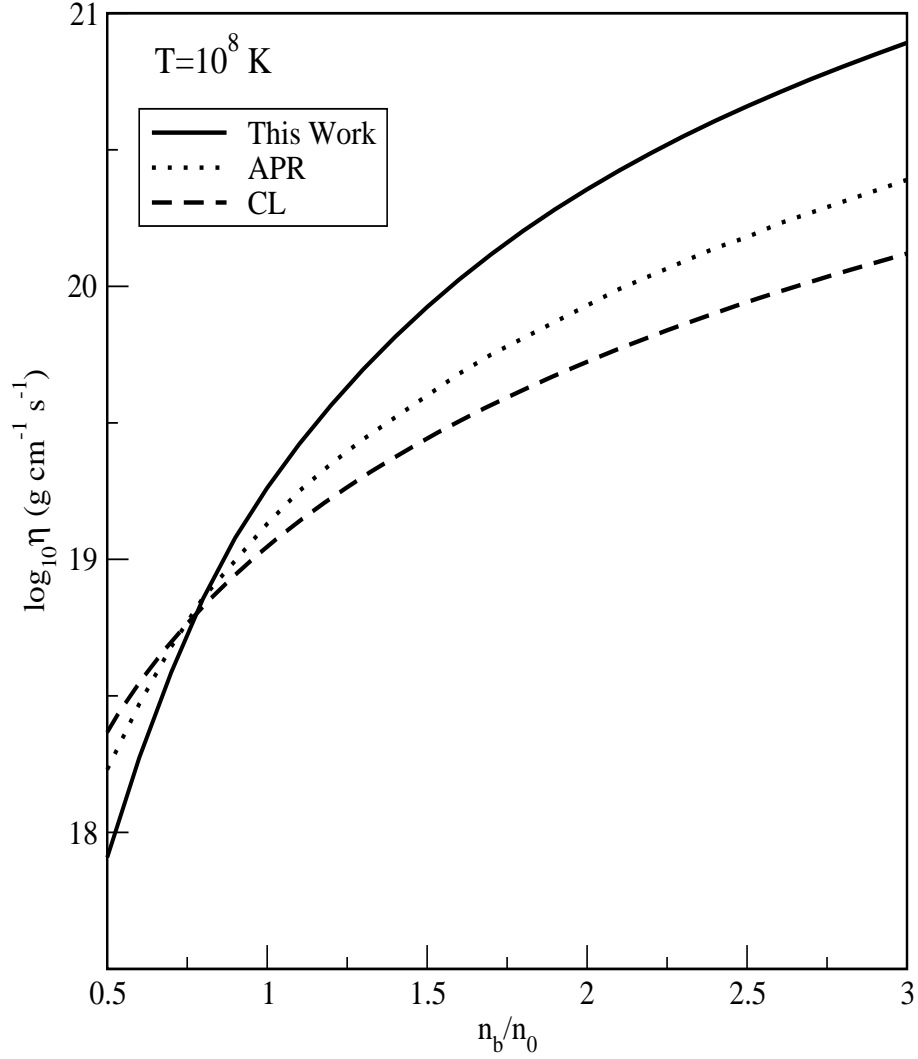


Fig. 4. Total shear viscosities in nuclear matter without an antikaon condensate corresponding to this work (solid line), the parameterization of Cutler and Lindblom (dashed line) and the EOS of Akmal, Pandharipande and Ravenhall are shown as a function of normalised baryon density at a temperature $T = 10^8$ K.

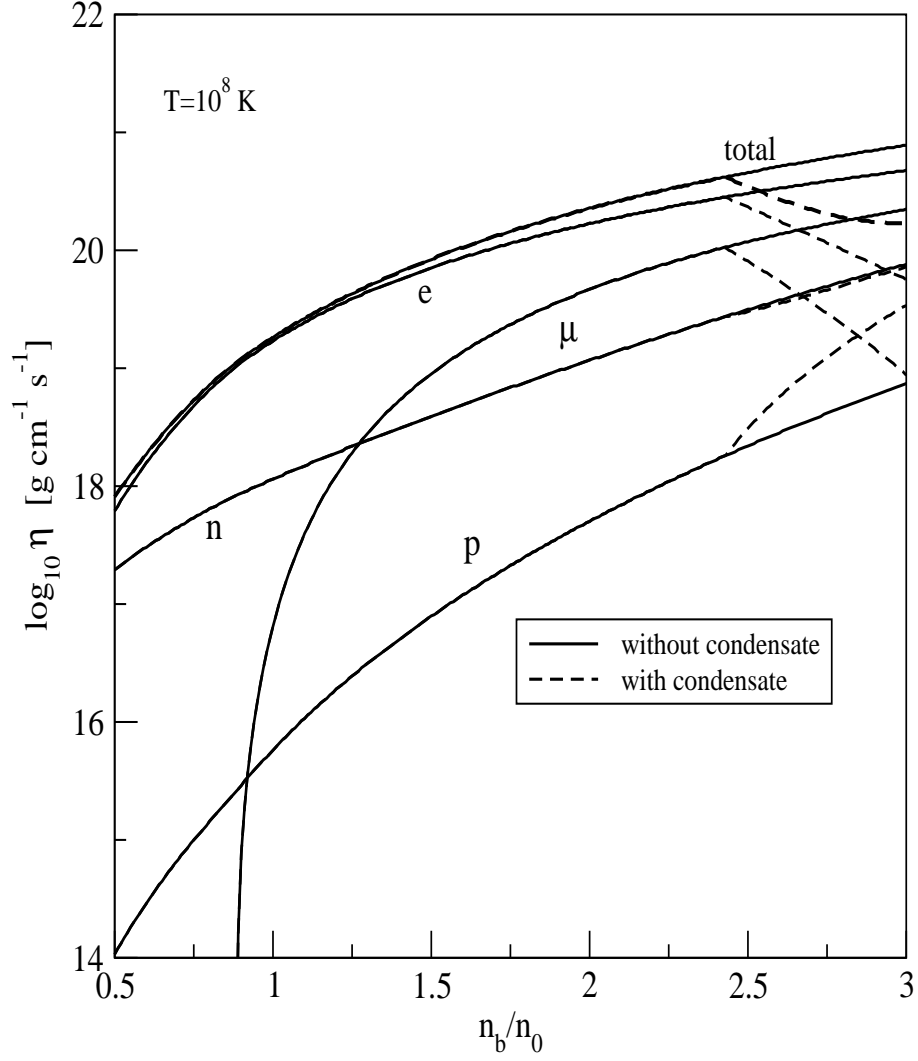


Fig. 5. The total shear viscosity as well as shear viscosities corresponding to different particle species are shown as a function of normalised baryon density at a temperature $T = 10^8 \text{ K}$ with (solid line) and without (dashed line) a K^- condensate.

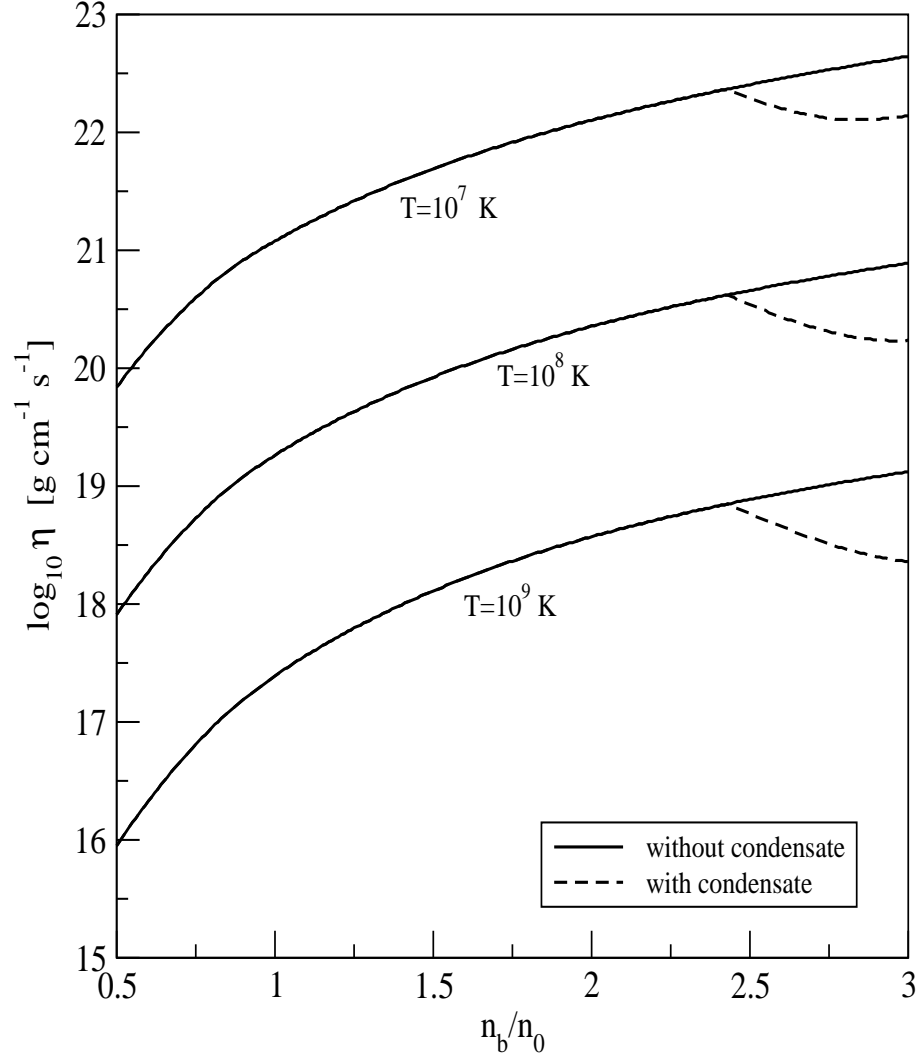


Fig. 6. The total shear viscosity as a function of normalised baryon density at different temperatures with (solid line) and without (dashed line) a K^- condensate.